

Periodic and purposely disordered superlattices: The effect of continuous and discrete disorder distribution

L. Pavesi* and F. K. Reinhart

Institut de Micro et -Optoélectronique, Ecole Polytechnique Fédérale, CH-1015 Lausanne, Switzerland

(Received 27 March 1990; revised manuscript received 4 June 1990)

Selective-excitation photoluminescence measurements were performed on purposely disordered superlattices to study the energy dependence of the motion of resonantly photocreated excitons in disordered superlattices. The disorder was introduced as a random succession of different well widths distributed according to a Gaussian function. We compare the continuous and the discrete Gaussian distributions of the disorder. In the latter case, we report the existence of different energy regions in the superlattice bands, corresponding to extended and spatially confined (localized) states. A calculation of the superlattice miniband spectrum and of the localization lengths for the different energy states suggests that the coupling between similar wells, although on different spatial regions, allows excitonic diffusion for some energies in the discrete Gaussian-disordered superlattice. According to calculations, a continuous Gaussian distribution yields only localized states.

In short-period superlattices (SL's) the coupling between adjacent wells leads to vertical (i.e., in the growth direction) transport through SL miniband states.¹ To study this transport by optical means, Chomette *et al.*² have proposed the use of an enlarged well (EW) (several monolayers wider than the SL well thickness) to detect the arrival of carriers at a certain distance from the surface.³ In addition, using selective-excitation photoluminescence (PL), the energy range in which carriers are created is controlled by selecting the energy of the exciting light, $\hbar\omega_{\text{ex}}$. Thus by scanning $\hbar\omega_{\text{ex}}$ through the electron-heavy-hole (*e-hh*) exciton emission band of the SL's and by looking at the emission from the EW, the spatial character of the states (extended or localized) of the *e-hh* pairs generated can be probed.⁴

During the molecular-beam-epitaxy (MBE) growth of SL's, controlled disorder can be introduced by variations of the growth parameters.⁵ By randomizing the SL well widths, it was shown that disorder inhibits the vertical transport at low temperatures.⁶ Moreover, this type of disorder modifies the energy miniband spectrum of the SL and different energy regions of extended and localized states appear.^{4,7} In a short-period SL, the coherence length of photoexcited electron-hole (*e-h*) pairs is at least five SL periods.⁸ Coupled to the effects of the purposely introduced disorder, the effects of uncontrolled statistical fluctuations in the composition of $\text{Al}_x\text{Ga}_{1-x}\text{As}$ barrier materials are present.⁹

The aim of this Brief Report is to compare two different kinds of disorder distributions. Samples with a discrete (*A*) (Ref. 10) or a continuous (*B*) (Ref. 11) random Gaussian distribution have been studied. Discrete Gaussian distribution is obtained by varying the well thickness of multiples of one monolayer (2.8 Å). For the continuous Gaussian distribution, the well thicknesses are changed by fractions of a monolayer. This is possible due to the average over the well interface fluctuations.

Figures 1(a) and 1(b) show the low-temperature PL spectra for the ordered samples *A*₁ and *B*₁, respectively.

The low-energy emissions are due to the excitonic (*ex*) recombination in the EW and the high-energy emissions are due to the *ex* recombination in the SL. We use as a measure of the number of excitons that move towards the EW the ratio $R = I_{\text{EW}}/I_{\text{tot}}$, where I_{EW} and I_{SL} are the integrated emission intensities of the EW and the SL, respectively, and $I_{\text{tot}} = (I_{\text{SL}} + I_{\text{EW}})$. For $\hbar\omega_{\text{ex}}$ at the high-energy side of the SL emission, R is equal to 0.7 and to 0.93 for samples *A*₁ and *B*₁, respectively. As both samples are periodic and contain no purposely introduced disorder, the ratio R is high. The difference in R could be ascribed to the uncontrolled interface fluctuations and/or to the alloy disorder present in the barriers. Moreover, the different growth parameters influence the efficiency of the vertical transport due to the different miniband widths of the heavy holes and electrons¹ (electron miniband width 53 or 73 meV and heavy-hole first miniband width 1.4 or 3 meV for sample *A*₁, $x = 35\%$, and sample *B*₁, $x = 25\%$, respectively).

The energy dependence of the ratio R is superimposed on the PL spectrum (solid points in Fig. 1). When $\hbar\omega_{\text{ex}}$ is resonant with the SL peak the transport toward the EW lowers. These experimental results suggest that the low-temperature PL of superlattices is mainly due to the emission of shallow localized excitons by interface fluctuations or alloy disorder in the barriers. This effect is also clearly observable on the excitation spectra performed on these samples (see, e.g., Ref. 12). When $\hbar\omega_{\text{ex}}$ is below the SL emission peak, R increases. It does not reach the value of 1 due to a resonantly enhanced emission of deeper localized states in the SL miniband. The two relative maxima shown in Fig. 1(a) at 1.694 and 1.707 eV reflect the heavy-hole and light-hole peaks in the absorption coefficient of sample *A*₁.

Figures 2(a) and 2(b) report the PL spectra of the purposely disordered samples *A*₂ and *B*₂ obtained with $\hbar\omega_{\text{ex}}$ higher than the first *e-hh* miniband edge. The high-energy peaks are the excitonic SL emissions and the low-

energy peak is due to carrier recombination within the EW. For sample A_2 , the high-energy peaks are centered around 1.68 eV, where the ordered sample has its SL emission. On the contrary, the SL emissions for sample B_2 are centered at a lower energy than in the ordered case (sample B_1). Let us note that by increasing the degree of disorder in samples of type B , i.e., increasing the standard deviation (σ) of the Gaussian distribution, the SL emission spectral region shifts from the ordered SL energies toward lower energies, eventually merging with the EW peak for a sample with a $\sigma \approx 8.9 \text{ \AA}$.⁶ As for the EW luminescence, the small difference in the EW spectral position for samples A_1 and A_2 , could be ascribed to unwanted different growth parameters (10 meV of difference corresponds to about 5 Å of variation in the well thickness for a 60-Å well).

By comparing Fig. 1 with Fig. 2, we find that the ratio R is lower in the case of the disordered samples due to a

reduction of the exciton vertical transport through the SL. Figure 2(a) shows that the number of excitons recombining in the EW depends on $\hbar\omega_{\text{ex}}$ for the disordered sample A_2 . We associate the fluctuations in R to the optical excitation of free or localized excitons (see Ref. 4 for a complete discussion of this experimental point). These features are not present in the disordered sample B_2 . $R(\hbar\omega_{\text{ex}})$ is almost independent on the excitation energy. Varying $\hbar\omega_{\text{ex}}$ there is a redistribution of intensity between the different SL emission lines, but no definitive evidence of energy regions with more mobile carriers is found. As the SL becomes transparent the ratio R increases for the two samples.

The density of states obtained by solving the Schrödinger equation for electrons and heavy holes¹³ is shown in Fig. 3 for samples A_2 and B_2 , respectively. [We have used the following material parameters (m_0 is the free-electron mass and x the aluminum concentra-

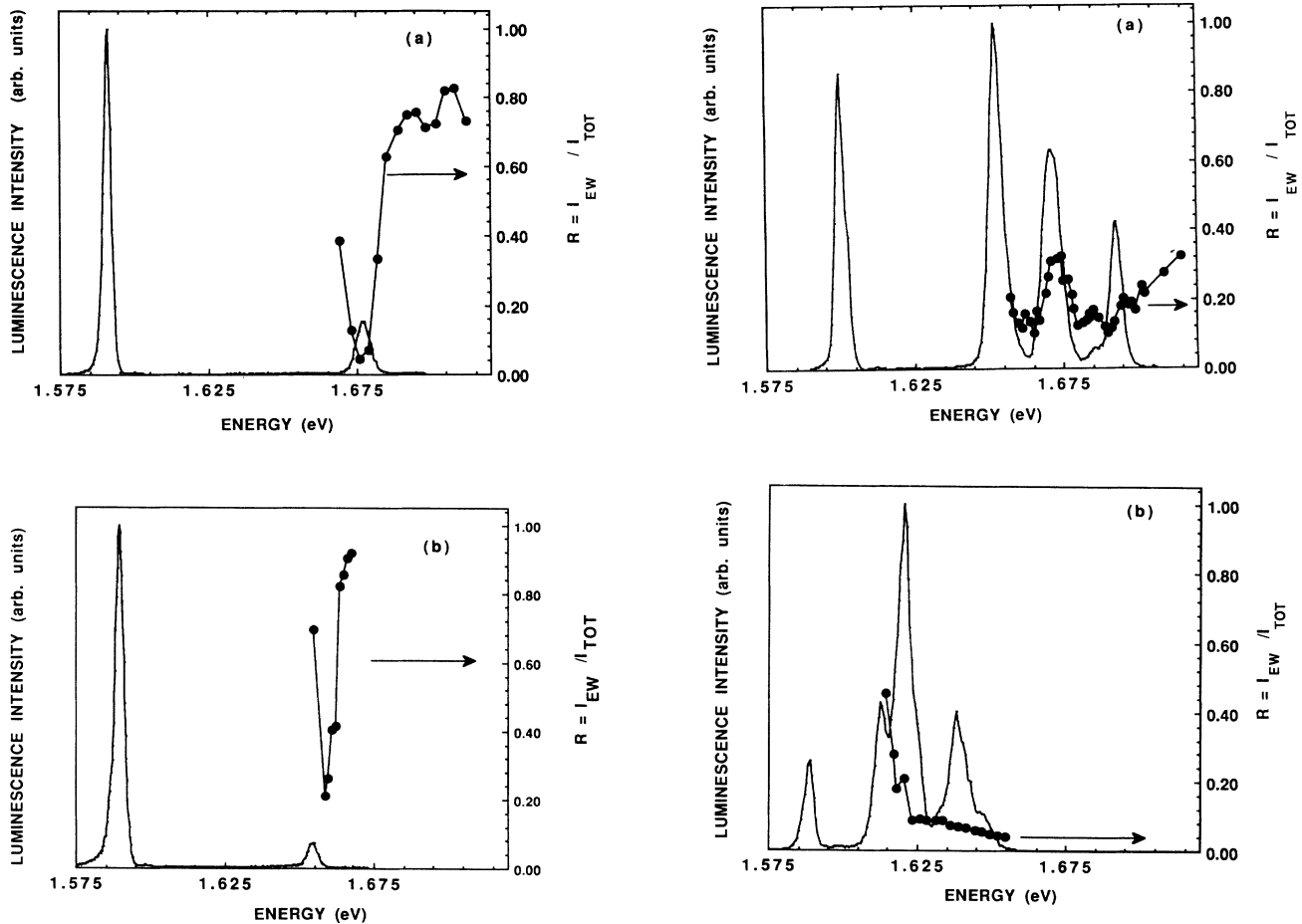


FIG. 1. Photoluminescence spectra at a bath temperature of 5 K of the ordered samples A_1 [part (a)] and B_1 [part (b)]. The excitation energy was 1.718 eV and the excitation intensity was 130 mW cm^{-2} . The solid points give the energy dependence of the ratio $R = I_{\text{EW}} / I_{\text{tot}}$, where I_{EW} and I_{SL} are the integrated emission intensities of the enlarged well and the superlattice, respectively, and $I_{\text{tot}} = (I_{\text{SL}} + I_{\text{EW}})$. The lines between the experimental points are only a guide for the eye.

FIG. 2. Photoluminescence spectra at a bath temperature of 5 K of the disordered samples A_2 [part (a)] and B_2 [part (b)]. The excitation energy was 1.718 eV for the spectrum (a) and 1.667 eV for the spectrum (b). The excitation intensity was 130 mW cm^{-2} . The solid points give the energy dependence of the ratio $R = I_{\text{EW}} / I_{\text{tot}}$, where I_{EW} and I_{SL} are the integrated emission intensities of the enlarged well and the superlattice, respectively, and $I_{\text{tot}} = (I_{\text{SL}} + I_{\text{EW}})$. The lines between the experimental points are only a guide for the eye.

tion): band gap $(1.5192 + 1.247x)$ eV; electron effective mass $(0.067 + 0.083x)m_0$; heavy-hole effective mass $(0.45 + 0.31x)m_0$; band offset $\Delta E_c = 0.62\Delta E_g$ (where ΔE_g and ΔE_c are the band-gap and conduction discontinuities between GaAs and $\text{Al}_x\text{Ga}_{1-x}\text{As}$.)] The minibands of electrons and heavy holes are broadened by the disorder for sample B_2 (dotted lines in Fig. 3). The spectral position of the SL emission in the disordered sample B_2 changes with respect to the ordered sample B_1 , because the photoexcited e - h pairs relax into the SL broadened minibands. Several peaks appear due to a spatial variation in the SL miniband edge which follows the random variation of well thicknesses. From our calculations, we

expect a low-energy shift of about 43 meV for the lowest luminescent emission of the SL (about 33 meV reduction in the SL miniband edge plus about 10 meV increase in the excitonic binding energy for quantum-well excitons with respect to SL excitons⁸). Indeed, the SL emission at the lowest energy in Fig. 2(b) is shifted by 42 meV with respect to the SL emission of Fig. 1(b). In the case of the disordered sample A_2 , the electron miniband is broadened too but the heavy-hole density of states shows different subbands separated by minigaps [indicated by arrows in Fig. 3(b)] inside the first broadened heavy-hole miniband. The discrete Gaussian disorder allows coupling between wells of the same thicknesses.⁴ The

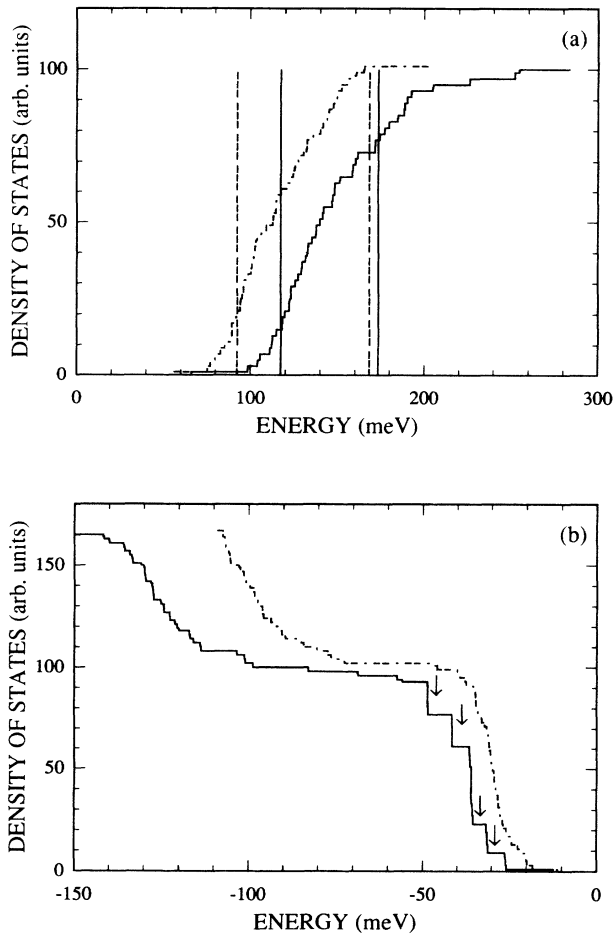


FIG. 3. Density of states (DOS) of the disordered samples A_2 (solid lines) and B_2 (dashed lines). (a) The electronic DOS; (b) the heavy-hole DOS. The energy scale is chosen to be zero at the bottom of the conduction band [part (a)] and at the top of the valence band [part (b)]. In part (a) the vertical solid lines show the electron miniband edges for the ordered superlattice A_1 and the vertical dotted lines show those for the ordered superlattice of type B_1 . In part (b) the arrows indicate the minigaps which are formed in the heavy-hole dispersion of the disordered sample A_2 . Let us note that the first heavy-hole miniband occurs at -39 meV for the ordered superlattice A_1 and at -34 meV for the ordered superlattice B_1 . The DOS for motion in the parallel direction has been taken as a step function.

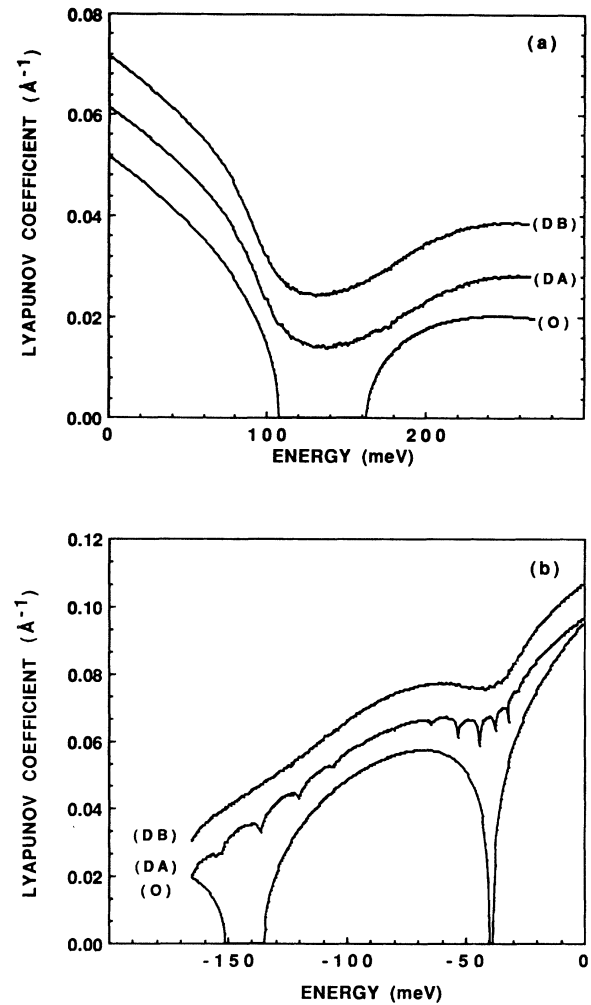


FIG. 4. Lyapunov coefficients as a function of the energy: (a) the electronic Lyapunov coefficient; (b) the heavy-hole Lyapunov coefficient. The label on the curves indicates (O) the ordered superlattice, (DA) the disordered superlattice A_2 , and (DB) the disordered superlattice B_2 . For this figure the superlattices A_2 and B_2 have been assumed with the same mean parameters changing only the Gaussian distribution: discrete for the A_2 results and continuous for the B_2 results. The energy scale is chosen to be zero at the bottom of the conduction band [part (a)] and at the top of the valence band [part (b)]. The curves DA are displaced by $+0.01 \text{\AA}^{-1}$ vertically and the curves DB by $+0.02 \text{\AA}^{-1}$ vertically to allow a better comparison.

luminescence is due to the recombination of excitons belonging to different subbands. Excitons formed by coupled quantum-well states could move somehow, and the diffusion depends on the energy of the photoexcited state.

Using the transfer-matrix method in one dimension,¹⁴ we calculate the Lyapunov exponents γ and the propagation probability $\tau(E) \approx e^{-\gamma(E)d}$ through the SL (where d is the SL thickness). $\gamma(E)$ represents the rate of exponential decay of the wave function of the state E and $1/\gamma(E)$ can be identified as its localization length.¹⁵ In the ordered case, Fig. 4, curve (O), $\gamma(E)$ goes to zero when E belongs to a miniband [$1/\gamma(E) \approx \infty$, extended state]. Consequently, $\tau(E)$ has a resonance whenever the state is extended. On the other hand, $\gamma(E)$ is always different from zero for the disordered SL. All the states are localized. The localization length is smaller for heavy holes [$1/\gamma(E) \approx 20$ Å for sample A_2 and $1/\gamma(E) \approx 17$ Å for sample B_2 when E belongs to the ordered SL hh subband] than for electrons [$1/\gamma(E) \approx 20$ Å for sample A_2 and 215 Å for sample B_2]. The effects of disorder on $\gamma(E)$ and, hence, on $\tau(E)$ are different for the heavy holes of the two disordered SL's. For sample B_2 , the result is a lessening and disappearance of the heavy-hole resonance [Fig. 4(b)

curve (DB)], whereas the subband structure is reflected in the appearance of several resonances in $\tau(E)$ for sample A_2 [Fig. 4(b) curve (DA)].

In conclusion, the effect of the disorder distribution on the excitonic vertical transport through purposely disordered SL's has been studied. For a continuous Gaussian distribution all the states are localized and the transport is inhibited. For a discrete Gaussian distribution coupling between wells of the same thickness is possible, even though they are placed in different sample regions. Excitons formed between single quantum-well-coupled states can tunnel. Hence transport throughout the SL is allowed for certain energies, although it is much less efficient than in the ordered case.

We acknowledge D. Martin and F. Morier-Genoud for the growth of samples of type A , and A. Regreny for the growth of samples of type B . Helpful discussions with A. Chomette and F. Clerot are acknowledged too. We thank E. Tuncel for her collaboration in an earlier phase of this work. This work was done in collaboration with Thomson-CSF.

*Present address: Department of Physics, University of Trento, I-38050 Povo (Trento), Italy.

¹B. Devaud, J. Shah, and T. C. Damen, Phys. Rev. Lett. **58**, 2582 (1987).

²A. Chomette, B. Deveaud, J. Y. Emery, and A. Regreny, Superlattices Microstruct. **1**, 201 (1985).

³B. Deveaud, J. Shah, T. C. Damen, B. Lambert, A. Chomette, and A. Regreny, IEEE J. Quantum Electron. **QE-24**, 1641 (1988).

⁴L. Pavesi, E. Tuncel, B. Zimmermann, and F. K. Reinhart, Phys. Rev. B **39**, 7788 (1989).

⁵S. D. Sarma, A. Kobayashi, and R. E. Prange, Phys. Rev. Lett. **56**, 1280 (1986).

⁶A. Chomette, B. Devaud, A. Regreny, and G. Bastard, Phys. Rev. Lett. **57**, 1464 (1986).

⁷E. Tuncel, L. Pavesi, D. Martin, and F. K. Reinhart, Phys. Rev. B **38**, 1597 (1988).

⁸E. E. Mendez, F. Agullo-Rueda, and J. M. Hong, Phys. Rev. Lett. **60**, 2426 (1988).

⁹E. Tuncel, L. Pavesi, and F. K. Reinhart, Superlattices Microstruct. **5**, 327 (1989).

¹⁰The samples of type A were grown at Ecole Polytechnique Fédérale de Lausanne in a 360 Varian MBE machine on n -type GaAs substrates. After a buffer layer (GaAs 500 Å, AlAs 100 Å, GaAs 4000 Å) and a superlattice with 30-Å-wide barrier of $\text{Al}_x\text{Ga}_{1-x}\text{As}$ and 30-Å-wide well of GaAs (49 periods), we grow an enlarged well (GaAs 60 Å) and then a superlattice (SL) different from one sample to the other. We have studied an ordered SL (sample A_1), which consists of 49 periods of 30-Å-wide $\text{Al}_x\text{Ga}_{1-x}\text{As}$ barriers and 30-Å-wide

GaAs wells, and a disordered SL (sample A_2), whose well thicknesses are random variables with a discrete Gaussian distribution (mean well width of 30 Å, standard deviation σ of 6 Å, and 2.8 Å of difference between the different possible values) and whose barriers are 30-Å-wide $\text{Al}_x\text{Ga}_{1-x}\text{As}$ layers. The aluminum content was always taken to be 35%. For more details, see D. Martin, E. Tuncel, F. Morier-Genoud, J. L. Staehli, and F. K. Reinhart, Helv. Phys. Acta **60**, 205 (1987).

¹¹The samples of type B were grown at Centre National d'Etudes des Télécommunications (Lannion) in a home modified MBE 500 Riber system. Each sample consists of (i) a GaAs buffer layer (1000 nm), (ii) a GaAs/ $\text{Al}_x\text{Ga}_{1-x}\text{As}$ SL1, (iii) a GaAs EW 64 Å wide, and (iv) superlattices SL2. SL1, and SL2 are identical and symmetrical with regard to EW. Also, for samples of type B we studied an ordered SL (49 periods of 30-Å-wide wells and barriers, sample B_1) and a disordered SL (sample B_2) with well widths, random variables, that follow a continuous Gaussian distribution with a mean value of 30 Å and standard deviation σ of 5.7 Å. The aluminum content was 25%. For more details see B. Deveaud, A. Regreny, J. Emery, and A. Chomette, J. Appl. Phys. **59**, 1633 (1986).

¹²A. Chomette, B. Lambert, B. Clerjaud, F. Clerot, H. W. Liu, and A. Regreny, Semicond. Sci. Technol. **3**, 351 (1988).

¹³B. Zimmermann-Piller, Ph.D. thesis, Ecole Polytechnique Fédérale de Lausanne, 1989.

¹⁴L. Pavesi and F. K. Reinhart, Phys. Status Solidi B **157**, 615 (1990).

¹⁵M. Kohomoto, Phys. Rev. B **34**, 5043 (1986).